Loss of Synchronized Retinal Phagocytosis and Age-related Blindness in Mice Lacking αvβ5 Integrin

Emeline F. Nandrot,[1] Yoonhee Kim,[1] Scott E. Brodie,[1,3] Xiaozhu Huang,[4] Dean Sheppard,[4] and Silvia C. Finnemann[1,2]

[1]*Margaret M. Dyson Vision Research Institute, Department of Ophthalmology, and* [2]*Department of Cell and Developmental Biology, Weill Medical College of Cornell University, New York, NY 10021*
[3]*Department of Ophthalmology, Mount Sinai School of Medicine, New York, NY 10029*
[4]*Lung Biology Center, Department of Medicine, University of California, San Francisco, San Francisco, CA 94143*

Abstract

Daily phagocytosis by the retinal pigment epithelium (RPE) of spent photoreceptor outer segment fragments is critical for vision. In the retina, early morning circadian photoreceptor rod shedding precedes synchronized uptake of shed photoreceptor particles by RPE cells. In vitro, RPE cells use the integrin receptor αvβ5 for particle binding. Here, we tested RPE phagocytosis and retinal function in β5 integrin–deficient mice, which specifically lack αvβ5 receptors. Retinal photoresponses severely declined with age in $\beta5^{-/-}$ mice, whose RPE accumulated autofluorescent storage bodies that are hallmarks of human retinal aging and disease. $\beta5^{-/-}$ RPE in culture failed to take up isolated photoreceptor particles. $\beta5^{-/-}$ RPE in vivo retained basal uptake levels but lacked the burst of phagocytic activity that followed circadian photoreceptor shedding in wild-type RPE. Rhythmic activation of focal adhesion and Mer tyrosine kinases that mediate wild-type retinal phagocytosis was also completely absent in $\beta5^{-/-}$ retina. These results demonstrate an essential role for αvβ5 integrin receptors and their downstream signaling pathways in synchronizing retinal phagocytosis. Furthermore, they identify the $\beta5^{-/-}$ integrin mouse strain as a new animal model of age-related retinal dysfunction.

Key words: circadian rhythm • knockout • photoreceptors • retinal pigment epithelium • vision

Introduction

Daily clearance phagocytosis by the retinal pigment epithelium (RPE) is essential for function and longevity of photoreceptor neurons. In the retina, photoreceptor rods and cones continuously renew their light-sensitive outer segments (1, 2). Circadian rhythms regulate photoreceptor outer segment turnover such that rods shed their most aged tips each morning with the onset of light, whereas cones shed their tips with the onset of night (3, 4). Early morning rod shedding precedes a synchronized burst of RPE phagocytosis, which rapidly clears shed photoreceptor outer segment fragments (POS) from the retina (5). Molecular mechanisms that RPE cells may use to coordinate their phagocytic response to shed POS are thus far unknown.

In the mammalian eye, RPE cells do not normally divide and each RPE cell underlies ∼30 photoreceptor cells.

Therefore, each individual RPE cell phagocytoses more material over a lifetime than any other cell type in the body. Even minor delays or inefficiencies in POS clearance by RPE cells will gradually cause accumulation of undigested photoreceptor components. Indeed, decline in RPE phagolysosomal processing is associated with the accumulation of storage bodies containing fluorescent lipofuscin, which is a complex mix of molecules rich in lipids that is characteristic for RPE aging in the human eye (6, 7). Excessive levels of lipofuscin are associated with retinal disease including the development of age-related macular degeneration, which is the leading cause of blindness among the elderly (8, 9).

The machinery used by RPE cells to phagocytose shed POS belongs to a family of related clearance mechanisms used by other cell types such as macrophages and dendritic

cells to phagocytose apoptotic cells (10). These mechanisms use common phagocyte surface receptors such as the Mer tyrosine kinase (MerTK; references 11–13), the scavenger receptor CD36 (14–17), and the integrin adhesive receptors αvβ3 and αvβ5 (16, 18–20). MerTK deficiency abolishes RPE's ability to internalize POS, which causes early onset retinal degeneration in the Royal College of Surgeons rat strain and in transgenic mice (11–13, 21–23). To our knowledge, phagocytosis by RPE lacking other phagocytic receptors has not been characterized to date.

Here, we explore β5 integrin–deficient mice to identify the effects of a permanent lack of αvβ5 integrin receptors on retinal and RPE function. Our results show that αvβ5 integrin deficiency is sufficient to cause age-related vision loss in $\beta5^{-/-}$ mice accompanied by accumulation of RPE lipofuscin, a cardinal feature of RPE aging and disease. Quantification of POS clearance demonstrates that lack of αvβ5 integrin primarily affects the phagocytic function of the RPE: $\beta5^{-/-}$ RPE in vitro fails to phagocytose POS and $\beta5^{-/-}$ RPE in vivo completely lacks the characteristic burst of phagocytosis in response to early morning rod shedding. Furthermore, our experiments identify a strict temporal regulation of focal adhesion kinase (FAK) and MerTK activities in the retina that correlates with circadian photoreceptor shedding. Strikingly, these synchronized signaling events are completely abolished in αvβ5-deficient retina. Together, these data provide the first direct evidence that αvβ5 integrin–dependent signaling is essential for retinal function by controlling RPE phagocytosis.

Materials and Methods

Animals. Previous characterization of $\beta5^{-/-}$ mice showed that these mice are viable and fertile, and they show no obvious morphologic abnormalities (24–26). $\beta5^{-/-}$ and wild-type mice of the same genetic background (129T2/SvEmsJ; The Jackson Laboratory) were housed under cyclic 12-h light/12-h dark light conditions (light onset at 6.00 h) and fed ad libitum. All procedures involving animals were approved by the Weill Medical College Institutional Animal Care and Use Committee.

For experiments, mice were killed by CO_2 asphyxiation. Lens and cornea were removed from enucleated eyeballs. Fresh eyecups were processed for microscopy or Western blotting as described below.

Electroretinography. Electroretinograms (ERGs) of five $\beta5^{-/-}$ and seven wild-type mice that were exactly age matched were recorded monthly between the ages of 4 and 12 mo. Mice were dark adapted overnight before anesthesia by i.p. injection of 100 mg/kg ketamine and 10 mg/kg xylazine. After topical eye anesthesia (0.5% proparacaine hydrochloride) and pupil dilation (10% phenylephrine hydrochloride and 1% tropicamide), full-field scotopic ERGs were recorded using a custom-made gold wire corneal contact lens electrode scaled to the mouse eye (provided by T. Mittag, Mount Sinai School of Medicine, New York, NY) and subdermal reference (forehead) and ground (back) electrodes as described previously (27). A photostimulator mounted in a reflective dome (Ganzfeld) was used to deliver 10-μs white flashes with full intensity flash stimuli of 1.5 cd-s/m² (UTAS-2000; LKC Technologies). Neutral density filters, ranging from −2.4 to 0 log neutral density filter (log ND) in 0.4 log unit steps were used to

decrease light stimuli. Stimuli were presented in order of increasing intensity. At least three separate responses were generated and presented as means ± SD for each of the seven intensities tested. A-wave amplitudes were measured from the baseline to the trough of the a-wave. B-wave amplitudes were measured from the trough of the a-wave to the peak of the b-wave.

Immunofluorescence and Light Microscopy. 10-μm-thick frozen sections from paraformaldehyde-fixed eyecups were prepared and stained with antibodies exactly according to established procedures (18, 28). For methyl green staining, 8-μm sections were cut from eyecups fixed in formalin/ethanol/acetic acid and embedded in paraffin. RGB light microscopy images were acquired using IP lab on a microscope (Axiovert 35; Carl Zeiss MicroImaging, Inc.) with a CCD camera (SenSys) and recompiled in Photoshop 7.0 (Adobe).

Cultured cells were fixed in ice-cold methanol and processed as described previously (29). Antibodies used were β5 integrin monoclonal antibody, polyclonal antibodies to β5 integrin (provided by L.F. Reichardt, University of California, San Francisco, San Francisco, CA) and to ZO-1 (Zymed). Secondary antibodies were purchased from Molecular Probes. Wide-field fluorescence images were acquired using MetaMorph (Universal Imaging) on an epifluorescence microscope (model C600; Nikon) with a cooled CCD camera (Princeton) or on a confocal microscopy system (model TSP2; Leica) and recompiled in Photoshop 7.0.

Electron Microscopy. Eyecups were fixed in 2.5% glutaraldehyde and 0.2% picric acid in 0.1 M cacodylate buffer, pH 7.3. Samples were post-fixed in 1% osmium tetroxide for 1 h, dehydrated in acetone, and embedded in Epon. Ultrathin sections were stained with uranyl acetate and lead citrate. Specimens were examined at 80 kV with an electron microscope (model 100 CXII; JEOL). Phagosomes were counted in electron micrographs of 0.5-μm retinal cross sections. For each time point and strain, three continuous stretches of RPE/photoreceptors of at least 1 mm in length, each prepared from different eyes, were examined. Structures were counted as phagosomes only if they (a) resided in the RPE cytoplasm and (b) contained lamellar membranes of the same appearance as those of intact photoreceptor outer segment tips in the same field.

Primary RPE Cell Culture. To isolate RPE from 12-d-old mice for primary culture, we adapted an experimental procedure previously used to harvest rat RPE (28). In brief, enucleated eyecups were treated with 1 mg/ml bovine hyaluronidase (Sigma-Aldrich) in Ca^{2+}-Mg^{2+}–free Hepes-buffered Hanks' saline (Cellgro) for 45 min to allow peeling off the neural retina and expose the RPE. After incubation was performed in 2 mg/ml trypsin (Difco) in Hepes-buffered Hanks' saline for 45 min, patches of RPE were peeled off manually from Bruch's membrane. Patches of purified RPE cells were seeded on serum-coated glass coverslips and grown in DMEM and 10% FBS at 37°C for 5–7 d before experiments.

POS Phagocytosis Assays. POS were isolated according to established protocols from bovine eyes obtained fresh from the slaughterhouse (18). Integrin inhibiting peptide GRGDSP and inactive control peptide GRADSP were purchased from Calbiochem. To determine POS binding or internalization, cells received POS covalently labeled with FITC dye (Molecular Probes; reference 18). Confluent RPE cells were challenged with ∼10 POS per cell in DMEM with 4% FCS for the duration of the experiment, chilled, washed three times with PBS containing 1 mM $MgCl_2$ and 0.2 mM $CaCl_2$ to remove excess POS, and lysed or fixed in ice-cold methanol. Nuclei were labeled with DAPI. Phagocytosed FITC-POS were quantified by fluorescence

microscopy using a wide-field setup (model E600; Nikon) with filters for FITC and DAPI. For each sample, phagocytosed (bound or internalized) POS in four separate fields of at least 20 cells each were counted. Duplicate samples were processed in each experiment. Three similar experiments were performed.

Cell Lysis and Immunoblotting. Cells were solubilized in 50 mM Hepes, pH 7.4, 150 mM NaCl, 10% glycerol, 1.5 mM $MgCl_2$, and 1% Triton X-100 that was freshly supplemented with 1% each of protease and phosphatase inhibitor cocktails (Sigma–Aldrich). Whole cell lysates representing 10,000 RPE cells or 10% of one mouse eyecup were immunoblotted using primary antibodies to FAK protein (C20; Santa Cruz Biotechnology, Inc.), FAK-P-Tyr-397 (Biosource), MerTK protein (RD systems), phospho-MerTK (Fabgennix) and RPE65 (provided by T.M. Redmond, National Eye Institute, Bethesda, MD), and to appropriate horseradish peroxidase–conjugated secondary antibodies; this was followed by ECL detection (PerkinElmer). X-ray films were scanned and signals quantified using NIH Image 1.61.

Results

Age-related Loss of Photoreceptor Function in β5 Integrin–deficient Mice. We used scotopic ERG recordings to compare photoreceptor function of $\beta5^{-/-}$ mice with that of strain-matched wild-type controls between 4 and 12 mo old. Retinal photoresponses significantly and progressively declined with age in $\beta5^{-/-}$ mice. Individual ERG recordings showed that single light flashes of different intensities elicited reduced a- and b-waves in $\beta5^{-/-}$ mice compared with wild-type mice at 12 mo (Fig. 1, a and b). Reduction of a-wave amplitudes in 12-mo-old $\beta5^{-/-}$ mice by up to 74% indicated a primary defect in rod photoreceptor function. To determine onset and progression of visual impairment of $\beta5^{-/-}$ mice, we performed ERG recordings of age-matched groups of wild-type and $\beta5^{-/-}$ mice from 4 to 12 mo old. All 4-mo-old $\beta5^{-/-}$ mice had normal vision (Fig. 1, c and d). Scotopic responses declined in all $\beta5^{-/-}$ mice after 4 mo old (Fig. 1 c). At 6 mo old, some $\beta5^{-/-}$ mice showed reduced photoresponses, whereas others were still normal. With advancing age, $\beta5^{-/-}$ mice became more similar to each other and more different from control mice (Fig. 1 c). In general, both a- and b-wave amplitudes significantly decreased with age in $\beta5^{-/-}$ mice, whereas those of wild-type controls remained mostly constant (Fig. 1 d). These results demonstrated that a lack of αvβ5 integrin caused late onset retinal dysfunction in mice.

Age Pigment Deposits in β5 Integrin–deficient Mice. Next, we compared retinal morphologies of $\beta5^{-/-}$ and wild-type mice. We confirmed that β5 integrin localized to the apical surface of the RPE in wild-type but not in $\beta5^{-/-}$ eyes (Fig. 2, a–d). Gross retinal morphology was similar in 1- and 12-mo-old mice of both strains (Fig. 2, compare a and b with e and f). However, at 12 mo old, $\beta5^{-/-}$, but not wild-type, RPE contained high numbers of vesicular auto-fluorescent storage bodies (Fig. 2, g and h). At the electron microscopic level, we observed more abundant inclusion bodies in RPE of $\beta5^{-/-}$ mice compared with wild-type mice (Fig. 2, i and j). Similar inclusion bodies are associated with incomplete turnover of POS-derived material and ac-
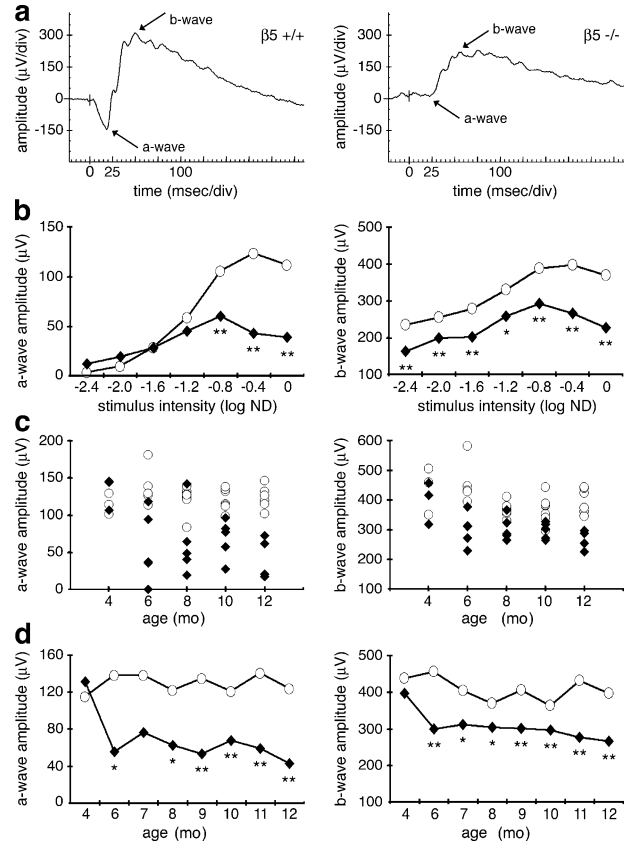
Figure 1. β5 integrin–deficient mice lose vision with age. We recorded scotopic ERG responses obtained after a light flash stimulus attenuated with 0.4 log ND (a, c, and d) or attenuated as indicated (b). We compared a-wave (left) and b-wave (right) amplitudes of control (open circles) and $\beta5^{-/-}$ (closed diamonds) mice. A-wave amplitudes are given as absolute values. (a) Representative ERG responses are diminished in 12-mo-old $\beta5^{-/-}$ mice (right) compared with wild-type mice (left). Both a- and b-wave peaks (arrows) are affected. (b) Mean scotopic responses to flashes of different intensities are decreased in 12-mo-old $\beta5^{-/-}$ mice. Asterisks indicate significant differences between wild-type and $\beta5^{-/-}$ amplitudes at the same flash intensity ($n = 5$–7, Student's t test, *, P < 0.05; **, P < 0.01). (c) Responses of individual animals (c) and of averages (d) illustrate decline of retinal function in $\beta5^{-/-}$ mice with age. Asterisks indicate significant differences between wild-type and $\beta5^{-/-}$ amplitudes at the same age ($n = 5$–7, Student's t test, *, P < 0.05; **, P < 0.01).

cumulate in aged and diseased retina. Excessive accumulation of autofluorescent storage bodies therefore suggested impaired POS turnover or phagocytosis by the RPE in β5 integrin–deficient mice.

Impaired POS Phagocytosis by β5 Integrin–deficient RPE. To directly test the phagocytic activity of $\beta5^{-/-}$ RPE, we performed in vitro phagocytosis assays. These allowed us to distinguish direct effects of β5 integrin knockout on phagocytic activity of RPE from secondary effects caused by altered photoreceptor shedding or photoreceptor–RPE interactions. $\beta5^{-/-}$ RPE cells in primary culture retained overall similar morphology and pigmentation as wild-type RPE (Fig. 3, a and d). Labeling with β5 antibody confirmed that wild-type, but not $\beta5^{-/-}$, RPE in culture continued to express abundant αvβ5 (Fig. 3, b and e). How-
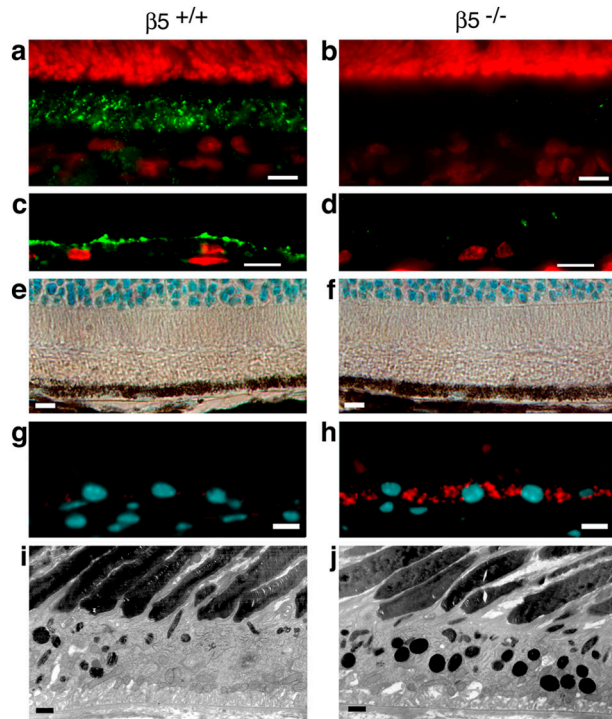
Figure 2. β5 integrin–deficient RPE accumulates autofluorescent lipofuscin with age. (a–d) Cryosections of 1-mo-old eyecups of wild-type (a and c) and $\beta5^{-/-}$ (b and d) mice were labeled with β5 antibody (green). Nuclei are shown in red. (a) In the wild-type mouse, whole retina sections with the neural retina present and β5 integrin was present in the photoreceptor outer segment layer, which also contains apical microvillar processes of RPE ensheathing photoreceptor outer segments (reference 28). (b) As expected, β5 integrin was absent from $\beta5^{-/-}$ retina. (c and d) To determine whether β5 integrin resided on photoreceptor outer segments or on RPE apical extensions, we prepared sections from eyecups from which the neural retina was peeled off before fixation. Prominent β5 integrin labeling at the apical surface of wild-type but not $\beta5^{-/-}$ RPE indicated that mouse RPE in vivo expresses apical αvβ5 integrin. (e–f) Methyl green–stained paraffin sections of eyecups from 12-mo-old wild-type (e) and $\beta5^{-/-}$ (f) mice were examined by light microscopy. Wild-type and $\beta5^{-/-}$ retina did not differ in appearance of photoreceptor nuclei (cyan at the top of the field), inner and outer segments (clear areas), and RPE (brown pigment and cyan nuclei). (g–h) Cryosections of eyecups from 12-mo-old wild-type (g) and $\beta5^{-/-}$ (h) mice were examined by wide-field fluorescence microscopy to detect DAPI-stained nuclei (cyan) and autofluorescence (detected in the rhodamine channel, red). $\beta5^{-/-}$, but not wild-type, RPE contained numerous autofluorescent inclusion bodies resembling the characteristic age pigment lipofuscin in human RPE (32). (i–j) Ultrathin sections of eyecups from 12-mo-old wild-type (i) and $\beta5^{-/-}$ (j) mice were examined by transmission electron microscopy. Increased presence of electron dense inclusion bodies in $\beta5^{-/-}$ RPE compared with wild-type RPE confirmed the results obtained by fluorescence microscopy. Bars: (a–h) 10 μm; (i and j) 1 μm.

ever, RPE from $\beta5^{-/-}$ mice phagocytosed fewer isolated POS than RPE from wild-type mice during 1 h of POS challenge (Fig. 3, c and f). Quantification of particle uptake revealed that loss of αvβ5 drastically reduced RPE phagocytosis of POS by ∼75% at all time points rather than delaying phagocytosis kinetics (Fig. 3 g). RGD peptides compete for ligand binding by many integrins including αvβ5. Sensitivity of wild-type, but not $\beta5^{-/-}$, RPE phagocytosis to RGD peptides therefore confirmed that wild-type, but
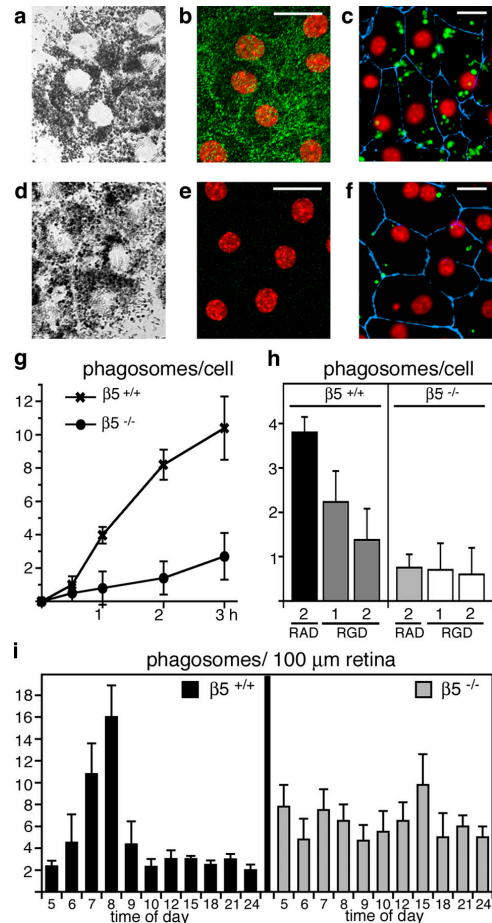
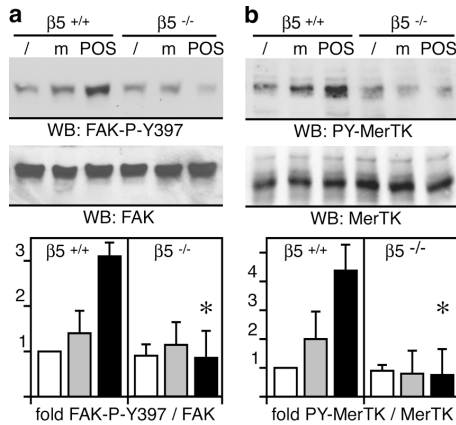**Figure 3.** Lack of αvβ5 integrin impairs RPE phagocytosis of POS. We examined primary RPE in culture from wild-type (a–c) and $\beta5^{-/-}$ (d–f) mice. Confocal x-y scans of transmitted light (a and d) and of apical αvβ5 integrin (green) and nuclei (red) in the same fields (b and e) were used to compare general cell morphology and to illustrate apical αvβ5 receptors in wild-type, but not in $\beta5^{-/-}$, RPE. (c and f) Junction marker ZO-1 (blue) and nuclei (red) appeared similar by wide-field fluorescence microscopy. However, $\beta5^{-/-}$ RPE in primary culture phagocytosed fewer FITC-POS (green) than wild-type RPE during a 1-h phagocytic challenge. (g) Quantification of in vitro phagocytosis assays showed reduced POS uptake by $\beta5^{-/-}$ RPE compared with wild-type RPE at all time points. Results represent means ± SD, n = 3, Student's t test, P < 0.01 at 1–3 h. (h) RGD peptides inhibited POS uptake by wild-type but not by $\beta5^{-/-}$ RPE in a concentration-dependent manner. Bars show 1-h FITC-POS uptake by wild-type and $\beta5^{-/-}$ RPE in the presence of 2 mM RAD-inactive control peptide, 1 or 2 mM integrin inhibiting RGD peptide as indicated. Since RGD peptides affected cell–substrate adhesion of both wild-type and $\beta5^{-/-}$ RPE at concentrations above 2 mM, these concentrations were not used for phagocytosis assays. Thus, the 63% inhibition we observed in the presence of 2 mM RGD peptide may not represent maximal possible inhibition of POS uptake by RGD peptides. Results represent means ± SD, n = 3, Student's t test, P < 0.01 for wild-type RPE, RGD versus RAD peptide at 2 mM. (i) Phagosome quantification in electron micrographs of retinal cross sections revealed that $\beta5^{-/-}$ retina lacked the characteristic burst of phagocytosis that followed the light onset (at 6.00 h) in wild-type retina. Mean (numbers of phagosomes) ± SD is shown. Sections from three eyecups per time point harvested in three separate experiments were examined.

not $\beta5^{-/-}$, RPE phagocytosis used αvβ5, which is the sole integrin at the apical phagocytic surface of RPE (Fig. 3 h; reference 18).

To determine the phagocytic activity of RPE cells in vivo, we counted the numbers of RPE phagosomes containing shed POS in electron microscopy images of cross sections of eyecups derived from wild-type and $\beta5^{-/-}$ mice at 3–4 wk old. As characteristic for normal retina, phagosome abundance increased promptly in wild-type RPE after the 6.00 h light onset, but was very low at all other times of day (Fig. 3 i, black bars). In stark contrast to normal RPE, $\beta5^{-/-}$ RPE completely lacked the phagocytic burst in response to circadian outer segment shedding, but it contained similar numbers of POS phagosomes at all times of day (Fig. 3 i, gray bars). Together, this quantification of POS phagocytosis by $\beta5^{-/-}$ RPE in vitro and in vivo demonstrated that a lack of $\alpha v\beta5$ integrin directly altered the phagocytic activity of RPE cells. Importantly, POS uptake was impaired in $\beta5$ integrin–deficient mice at a young age when vision was still normal (Fig. 1).

$\beta5$ Integrin–deficient RPE Cells in Culture Fail to Activate FAK and MerTK upon POS Challenge. Our previous studies attributed an essential signaling response to POS challenge involving FAK and MerTK in rat RPE to signaling downstream of $\alpha v\beta5$ integrin (29). Therefore, we determined levels of tyrosine phosphorylation of FAK and MerTK that usually imply activation of these kinases. 1 h phagocytic challenge with isolated POS but not with assay medium alone increased phosphorylation at FAK's autophosphorylation site tyrosine 397 (Y397) in wild-type mouse RPE in culture 3.1-fold (Fig. 4 a). Similarly, POS specifically increased MerTK tyrosine phosphorylation 4.4-fold (Fig. 4 b). In contrast, $\beta5^{-/-}$ RPE cells did not respond to POS challenge with phosphorylation of either FAK or MerTK (Fig. 4, a and b). Absence of FAK and MerTK phosphorylation was not caused by lower levels of expression of these kinases as immunoblotting showed similar steady-state amounts of these proteins in wild-type and $\beta5^{-/-}$ RPE.

$\beta5$ Integrin–deficient Mice Lack In Vivo Phagocytic Signaling. Finally, we set out to test whether retinal phagocytosis in vivo also involved signaling pathways using FAK and MerTK. We harvested eyecups from age-matched, 3-wk-old wild-type and $\beta5^{-/-}$ mice in 1.5-h intervals from 1 h before light onset (5.00 h) until 11.00 h and at 18.00 h. Fig. 5 shows that FAK and MerTK tyrosine phosphorylation levels in wild-type eyecups promptly increased after light onset and peaked at 6.30 h and 8.00 h, respectively, the period of the daily phagocytic burst of RPE (Fig. 3 i). In contrast,
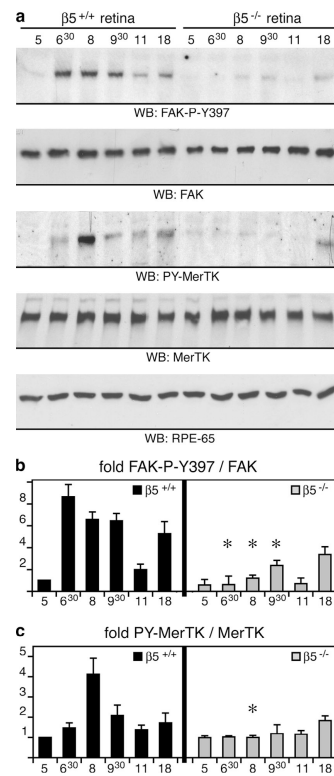
Figure 5. $\beta5$ integrin–deficient retina lacks synchronized activation of FAK and MerTK. (a) Eyecup detergent lysates were prepared from 3-wk-old wild-type and $\beta5^{-/-}$ mice at different times of the day, as indicated. Expression and phosphorylation profiles of proteins were compared by immunoblotting with primary antibodies as indicated in the panels. (b and c) Specific activities of FAK and MerTK were determined as in Fig. 4. Promptly after light onset, levels of active, phosphorylated FAK and MerTK increased in wild-type eyecups. This increase was absent in $\beta5^{-/-}$ eyecups. Similar results were obtained comparing expression and activity profiles of FAK and MerTK in wild-type and $\beta5^{-/-}$ mice at 7 and 12 mo (unpublished data). Note that the rise in FAK phosphorylation preceded the increase of MerTK phosphorylation. This agreed well with our earlier data from in vitro phagocytosis assays showing that MerTK activation upon POS challenge requires FAK activation (reference 29). Ratios of active, phosphorylated protein/total protein are given as fold change compared with ratios in wild-type eyes at 5.00 h, which were set at 1.0 arbitrarily. Results are presented as means ± SD. Asterisks indicate significant differences in ratios ($n = 3$, Student's t test, $P < 0.05$) between wild-type and $\beta5^{-/-}$ samples at the same time points.

Figure 4. $\beta5$ integrin–deficient RPE in culture fails to activate phagocytic signaling. (a) Primary wild-type and $\beta5^{-/-}$ RPE in culture were untreated (lanes /) or received assay medium (lanes m) or POS in assay medium (lanes POS) for 1.5 h. Lysates normalized for RPE protein content were analyzed by immunoblotting with antibodies specific for FAK-P-Y397 and FAK protein. Specific activity of FAK is given as a ratio of FAK-P-Y397 to total FAK and given as fold change compared with untreated wild-type RPE. ($n = 3$). (b) The same experiment was performed to determine changes in MerTK activity. Specific activity of MerTK is given as a ratio of PY-MerTK to total MerTK and given as fold change compared with untreated wild-type RPE. (a and b) Results are presented as means ± SD. Asterisks indicate significant differences in ratios between wild-type and $\beta5^{-/-}$ samples of the same treatment (Student's t test, $P < 0.001$).

$\beta5^{-/-}$ eyecups retained basal levels of FAK and MerTK tyrosine phosphorylation at all times (Fig. 5, a–c). Protein expression levels remained constant and were the same in both wild-type and $\beta5^{-/-}$ eyecups. Equal levels of the RPE-specific protein RPE65 confirmed that all eyecup samples represented the same number of RPE cells (Fig. 5 a).

Thus, FAK and MerTK activation during POS phagocytosis by RPE in vitro completely correlated with rhythmic activation of these kinases during retinal phagocytosis in vivo. Together, these results strongly suggested that MerTK and FAK activation in whole eyecups at the peak of daily phagocytic activity reflected rhythmic phagocytic signaling by RPE cells in the retina. Furthermore, a lack of these signaling pathways in β5-deficient RPE indicated that they required αvβ5 integrin.

Discussion

This study provides the first demonstration that a lack of αvβ5 integrin impairs a form of noninflammatory clearance phagocytosis in vivo. Our results suggest that peak activity of the RPE's engulfment machinery requires αvβ5 integrin–dependent signaling pathways via FAK and MerTK. This signaling mechanism is essential for long-term function of photoreceptors.

Our data show that RPE cells use αvβ5 integrin–dependent signaling to synchronize their unique rhythmic phagocytic activity with the circadian rhythm of photoreceptor shedding in the retina. In vitro evidence has long suggested that macrophages and dendritic cells, like RPE cells, use αvβ3 or αvβ5 integrin receptors to phagocytose spent cells undergoing apoptosis (10, 16, 20). Furthermore, a lack of functional MerTK impairs both engulfment of spent cells by macrophages and engulfment of spent POS by RPE (13, 23). Together, these results suggest that integrin downstream signaling pathways may also serve to acutely increase engulfment capacity of other phagocytic cells such as macrophages to ensure rapid and efficient clearance of apoptotic cells.

In vivo and in vitro POS–RPE interactions differ significantly from each other, as POS are always in contact with RPE cells in the retina, but de novo binding by POS must precede engulfment in in vitro assays. However, our results show that RPE in vivo and in vitro activate identical signaling pathways to POS phagocytic challenge. This implies a primary role for αvβ5 integrin in RPE function as an important signaling protein that initiates and controls the in vivo rhythm of POS phagocytosis by the RPE.

Our results identify a defect in RPE phagocytosis that causes age-related blindness in mice lacking αvβ5 integrin. $\beta5^{-/-}$ mice lacked synchronized POS phagocytosis even at a young age immediately after retinal maturation. In contrast, photoreceptor function in these mice decreased only when they were >4 mo old. Similarly, only RPE of old $\beta5^{-/-}$ mice revealed accumulation of autofluorescent age lipids. This suggests that the altered time course of POS uptake by RPE is the primary effect of β5 integrin defi-ciency in the retina. It further demonstrates that basal levels of POS phagocytosis in $\beta5^{-/-}$ mice suffice to clear shed POS from the retina within 24 h, thus preventing buildup of shed POS, which causes rapid damage to retinal photoreceptors (21, 22, 30). However, accumulation of autofluorescent storage lipids we detected in $\beta5^{-/-}$ mice of age indicates that engulfed POS are likely processed incompletely by $\beta5^{-/-}$ RPE cells. We suggest that such differences in phagolysosomal digestion of POS material may account for secondary effects on photoreceptor function causing the age-dependent vision loss in $\beta5^{-/-}$ mice. Fluorescent lipofuscin accumulation is a common characteristic of aging and of many forms of disease in the human retina (9). Our data support earlier evidence that suggested a direct link of altered photoreceptor POS turnover and lipofuscin accumulation by the RPE (31). They further validate the $\beta5^{-/-}$ mouse strain as a valuable animal model for studies of retinal aging. Future studies will explore how environmental or additional genetic factors may contribute to onset, progression, and severity of retinal defects in mice that lack αvβ5 integrin.

References

1. Young, R.W. 1967. The renewal of photoreceptor cell outer segments. *J. Cell Biol.* 33:61–72.
2. Young, R.W. 1971. The renewal of rod and cone outer segments in the rhesus monkey. *J. Cell Biol.* 49:303–318.
3. LaVail, M.M. 1976. Rod outer segment disk shedding in rat retina: relationship to cyclic lighting. *Science.* 194:1071–1074.
4. Young, R.W. 1977. The daily rhythm of shedding and degradation of cone outer segment membranes in the lizard retina. *J. Ultrastruct. Res.* 61:172–185.
5. Young, R.W., and D. Bok. 1969. Participation of the retinal pigment epithelium in the rod outer segment renewal process. *J. Cell Biol.* 42:392–403.
6. Feeney, L. 1978. Lipofuscin and melanin of human retinal pigment epithelium. Fluorescence, enzyme cytochemical, and ultrastructural studies. *Invest. Ophthalmol. Vis. Sci.* 17:583–600.
7. Feeney-Burns, L., and G.E. Eldred. 1983. The fate of the phagosome: conversion to 'age pigment' and impact in human retinal pigment epithelium. *Trans. Ophthalmol. Soc. U.K.* 103:416–421.
8. Holz, F.G., C. Bellman, S. Staudt, F. Schutt, and H.E. Vol-

cker. 2001. Fundus autofluorescence and development of geographic atrophy in age-related macular degeneration. *Invest. Ophthalmol. Vis. Sci.* 42:1051–1056.

9. von Ruckmann, A., F.W. Fitzke, and A.C. Bird. 1997. In vivo fundus autofluorescence in macular dystrophies. *Arch. Ophthalmol.* 115:609–615.

10. Finnemann, S.C., and E. Rodriguez-Boulan. 1999. Macrophage and retinal pigment epithelium phagocytosis: apoptotic cells and photoreceptors compete for αvβ3 and αvβ5 integrins, and protein kinase C regulates αvβ5 binding and cytoskeletal linkage. *J. Exp. Med.* 190:861–874.

11. D'Cruz, P.M., D. Yasumura, J. Weir, M.T. Matthes, H. Abderrahim, M.M. LaVail, and D. Vollrath. 2000. Mutation of the receptor tyrosine kinase gene Mertk in the retinal dystrophic RCS rat. *Hum. Mol. Genet.* 9:645–651.

12. Nandrot, E., E.M. Dufour, A.C. Provost, M.O. Pequignot, S. Bonnel, K. Gogat, D. Marchant, C. Rouillac, B. Sepulchre de Conde, M.T. Bihoreau, et al. 2000. Homozygous deletion in the coding sequence of the c-mer gene in RCS rats unravels general mechanisms of physiological cell adhesion and apoptosis. *Neurobiol. Dis.* 7:586–599.

13. Scott, R.S., E.J. McMahon, S.M. Pop, E.A. Reap, R. Caricchio, P.L. Cohen, H.S. Earp, and G.K. Matsushima. 2001. Phagocytosis and clearance of apoptotic cells is mediated by MER. *Nature.* 411:207–211.

14. Ren, Y., R.L. Silverstein, J. Allen, and J. Savill. 1995. CD36 gene transfer confers capacity for phagocytosis of cells undergoing apoptosis. *J. Exp. Med.* 181:1857–1862.

15. Ryeom, S.W., J.R. Sparrow, and R.L. Silverstein. 1996. CD36 participates in the phagocytosis of rod outer segments by retinal pigment epithelium. *J. Cell Sci.* 109:387–395.

16. Albert, M.L., S.F.A. Pearce, L.M. Francisco, B. Sauter, P. Roy, R.L. Silverstein, and N. Bhardwaj. 1998. Immature dendritic cells phagocytose apoptotic cells via αvβ5 and CD36, and cross-present antigens to cytotoxic T lymphocytes. *J. Exp. Med.* 188:1359–1368.

17. Finnemann, S.C., and R.L. Silverstein. 2001. Differential roles of CD36 and αvβ5 integrin in photoreceptor phagocytosis by the retinal pigment epithelium. *J. Exp. Med.* 194:1289–1298.

18. Finnemann, S.C., V.L. Bonilha, A.D. Marmorstein, and E. Rodriguez-Boulan. 1997. Phagocytosis of rod outer segments by retinal pigment epithelial cells requires αvβ5 integrin for binding but not for internalization. *Proc. Natl. Acad. Sci. USA.* 94:12932–12937.

19. Miceli, M.V., D.A. Newsome, and D.J. Tate Jr. 1997. Vitronectin is responsible for serum-stimulated uptake of rod outer segments by cultured retinal pigment epithelial cells. *Invest. Ophthalmol. Vis. Sci.* 38:1588–1597.

20. Savill, J., I. Dransfield, N. Hogg, and C. Haslett. 1990. Vitronectin receptor-mediated phagocytosis of cells undergoing apoptosis. *Nature.* 343:170–173.

21. Bok, D., and M.O. Hall. 1971. The role of the pigment epithelium in the etiology of inherited retinal dystrophy in the rat. *J. Cell Biol.* 49:664–682.

22. Mullen, R.J., and M.M. LaVail. 1976. Inherited retinal dystrophy: primary defect in pigment epithelium determined with experimental rat chimeras. *Science.* 192:799–801.

23. Duncan, J.L., M.M. LaVail, D. Yasumura, M.T. Matthes, H. Yang, N. Trautmann, A.V. Chappelow, W. Feng, H.S. Earp, G.K. Matsushima, and D. Vollrath. 2003. An RCS-like retinal dystrophy phenotype in mer knockout mice. *Invest. Ophthalmol. Vis. Sci.* 44:826–838.

24. Huang, X., M. Griffiths, J. Wu, R.V. Farese Jr., and D. Sheppard. 2000. Normal development, wound healing, and adenovirus susceptibility in β5-deficient mice. *Mol. Cell. Biol.* 20:755–759.

25. Reynolds, L.E., L. Wyder, J.C. Lively, D. Taverna, S.D. Robinson, X. Huang, D. Sheppard, R.O. Hynes, and K.M. Hodivala-Dilke. 2002. Enhanced pathological angiogenesis in mice lacking β3 integrin or β3 and β5 integrins. *Nat. Med.* 8:27–34.

26. Eliceiri, B.P., X.S. Puente, J.D. Hood, D.G. Stupack, D.D. Schlaepfer, X.Z. Huang, D. Sheppard, and D.A. Cheresh. 2002. Src-mediated coupling of focal adhesion kinase to integrin αvβ5 in vascular endothelial growth factor signaling. *J. Cell Biol.* 157:149–160.

27. Bayer, A.U., P. Cook, S.E. Brodie, K.P. Maag, and T. Mittag. 2001. Evaluation of different recording parameters to establish a standard for flash electroretinography in rodents. *Vision Res.* 41:2173–2185.

28. Bonilha, V.L., S.C. Finnemann, and E. Rodriguez-Boulan. 1999. Ezrin promotes morphogenesis of apical microvilli and basal infoldings in retinal pigment epithelium. *J. Cell Biol.* 147:1533–1548.

29. Finnemann, S.C. 2003. Focal adhesion kinase signaling promotes phagocytosis of integrin-bound photoreceptors. *EMBO J.* 22:4143–4154.

30. Dowling, J.E., and R.L. Sidman. 1962. Inherited retinal dystrophy of the rat. *J. Cell Biol.* 14:73–109.

31. Rakoczy, P.E., D. Zhang, T. Robertson, N.L. Barnett, J. Papadimitriou, I.J. Constable, and C.M. Lai. 2002. Progressive age-related changes similar to age-related macular degeneration in a transgenic mouse model. *Am. J. Pathol.* 161:1515–1524.

32. Finnemann, S.C., L.W. Leung, and E. Rodriguez-Boulan. 2002. The lipofuscin component A2E selectively inhibits phagolysosomal degradation of photoreceptor phospholipid by the retinal pigment epithelium. *Proc. Natl. Acad. Sci. USA.* 99:3842–3847.